Asian Journal of Chemistry; Vol. 34, No. 7 (2022), 1644-1652

ASIAN JOURNAL OF CHEMISTRY

https://doi.org/10.14233/ajchem.2022.23613

Density Functional Theory and Antimicrobial Studies on *tris*(*N*-Furfuryl-*N*-benzyldithiocarbamato-S,S′)antimony(III)

SUNDARAMOORTHY TAMILVANAN

Department of Chemistry, Annamalai University, Annamalai Nagar-608002, India

Corresponding author: E-mail: laksuntam@gmail.com

Received: 10 November 2021; *Accepted*: 18 January 2022; *Published online*: 15 June 2022; AJC-20835

In present work, the complex, *tris*(*N*-furfuryl-*N*-benzyldithiocarbamato-S,S′)antimony(III) has been synthesized and characterized by elemental analysis, IR, ^{1}H NMR, ^{13}C NMR and biological studies. In the theoretical calculations, the DFT method with the B3LYP hybrid functional using the LAN2DZ basis set has been selected as a computational technique. The molecular structure and spectral are explained by Gaussian computational analysis theory (B3LYP) are found to be in correlation with the experimental data observed from the various spectrophotometric methods. ^{1}H NMR and ^{13}C NMR were performed by using GIAO (Gauge Independent Atomic Orbital) process with the B3LYP method and the LAN2DZ basis set and NMR chemical shifts related to TMS were compared. The molecular orbital calculations such as HOMO-LUMO energy gap, Mulliken population analysis and MEP surfaces have been calculated. Further, the synthesized antimony dithicarbamate complex has been evaluated for *in vitro* antimicrobial activity against various microorganisms using the disc diffusion method. The results represented that the studied molecule has shown the antimicrobial activity.

Keywords: Dithiocarbamate, Antimony, DFT, MEP, Gauge independent atomic orbital.

INTRODUCTION

Antimony-based drugs are the front-line drugs against the protozoan parasite Leishmania in several countries [1]. Medicinal use of antimony complexes dates back to the 17th century, antimony(III) potassium tartrate was used to cure numerous diseases, like typhoid, snail fevers and lung diseases, *etc*. [2]. Recently, three antimonials are under clinical use, *i.e.* glucantime, stibophen and pentostam the latter being recommended by the world health organization (WHO) as the first choice drug against all types of leishmaniasis [3-8]. The analytical aspects of dithiocarbamate have been reviewed by several researchers [9-11] and their structural aspects have been reviewed by Tiekink [12]. The reviews by other researchers [13-15] cover the major facets of the metal dithiocarbamate complexes and related systems. Willemse *et al.* [16] reviewed the transition metal complexes of dithiocarbamates in curious oxidation states. Similarly, Steggerda *et al.* [17] also reviewed the metal complexes of dithiocarbamates and its related ligands, whereas the electrochemistry and redox behaviour of transition metal dithiocarbamates is reported by Martin & Bond [18].

Dithiocarbamate ligands with many wide range applications in materials science, antimicrobial agents, antioxidants, antitumor drugs, antiviral agents, pesticides, antidotes for phytotoxic substances, bactericides and antihumidity agents [19]. Dithiocarbamates are also adaptable chemical moieties with significant bonding and coordinating affinity to main group metal atoms [20-30]. However, 1,1-dithiochelates of main group elements are fewer widely explored than that of transition elements, especially the synthesis and structures of antimony(III) dithiocarbamate complexes. Metal dithiolates in meticulous have been used as single-source precursors in CVD and other related methods for the preparation of thin films of semiconductor materials in the past [31-33]. Metal dithiobiurets, dithiolates, alkoxides and diketonates like many metallo-organic compounds are used as precursors for optical and electronic properties [34-36]. On the other hand, antimony dithiocarbamate complexes have been reported with good antitumor activities and cytotoxicity, especially Wang *et al*. [37] reported some antimony dithiocarbamate complexes to affect the repair of DNA-double strand break. Antimony(III) chalcogenides, Sb_2X_3, where X = S and Se show excellent semiconducting

properties, photoconductivity and are potential applications in solar energy conversion. Experimental methods were adopted for the preparation of the chalcogenides outcome in the desired morphologies [38,39].

Diethyldithiocarbamates can inhibitory benzo[*a*]pyrene-induced tumors, while metal dithiocarbamate ligands have been investigated for their anticancer potential, remarkably with palladium(II), gold(I/III), platinum(IV) *bis*muth(III) and tin(IV) [40]. Antimony complexes with sulfur contain ligands the two polymorphic compounds of dimethyldithiocarbamate show the higher activity against MCF-7 cells [41-46]. These complexes exhibited higher activity than the typical anticancer agents such as doxorubicin [47], cisplatin [42,43] and tamoxifen [46]. Of note that they exhibited 158-340 fold higher activity against MCF-7 cells than cisplatin [41] and 21-53 fold higher activity against HeLa cells. Pyrrolidinedithiocarbamate contains a five-member ring attached to its nitrogen atom. In ethylene-*bis*-dithiocarbamates, two (NCS_2) moieties are bridged by ethylene. Transition metal dithiocarbamates generally exhibit higher antibacterial activities than the parent ligands [48].

Present work is concerned with the synthesis of antimony(III) complex containing furfuryl based dithiocarbamate ligand. Antimony(III) complex has been prepared from secondary amine by reaction with carbon disulfide and a corresponding metal salt. The elemental analyses, IR and NMR (^{1}H & ^{13}C NMR) spectra have been used in addition to conventional chemical methods to characterize the complex. Newly synthesized antimony(III) dithiocarbamate complex has been evaluated for their *in vitro* antibacterial activity against *Vibrio cholerae, Klebsiella pneumoniae, Escherichia coli* and *Staphylococcus aureus* and antifungal activity against *Aspergillus niger* and *Candida albicans*.

EXPERIMENTAL

Antimony trichloride, the parent amines, reagents and the solvents were of analytical grade (commercially available) materials and used as supplied without further purification. Melting points of the complexes were determined with a thermal melting point apparatus and used with open capillary tubes. Elemental analyses (C, H & N) were carried out with an Elementar Analyse Systeme Gmbh Vario El V3.00 at Sophisticated Analytical Instrument Facility Centre, CDRI, Lucknow, India. FT-IR spectra were recorded on Thermo Shimadzu FT-IR spectrophotometer (4000-400 cm^{-1}) as KBr pellets. ^{1}H NMR and ^{13}C NMR spectra were recorded on a BRUKER 400 MHz spectrometer model at room temperature using $CDCl_3$ as the solvent. The Bruker spectrometer was performed at 400 MHz for ^{1}H NMR spectra and 100 MHz for ^{13}C NMR spectra.

Synthesis of antimony(III) dithiocarbamate complex: Furfuraldehyde and benzylamine were dissolved in MeOH and the solution was stirred for 2 h at room temperature. The solvent was removed by evaporation. The resulting oily product was dissolved in a methanol-dichloromethane (1:1, 20 mL) solvent mixture. To this solution, sodium borohydride ($NaBH_4$) was added very slowly at 5 ºC and stirred for 2 h. The reaction product was stirred for 12 h at room temperature. After evaporation of solvent, the resulting viscous product was washed with water and dichloromethane was added to extract the product of secondary amine. Evaporation of organic layer product was *N*-furfuryl-*N*-benzylamine as yellow oil [49].

Preparation of *tris*(*N*-furfuryl-*N*-benzyldithiocarbamato-S,S′)antimony(III): *N*-Furfuryl-*N*-benzylamine and carbon disulfide were dissolved in ethanol and stirred for 30 min kept under ice-cold conditions (5 ºC) to obtain a yellow dithiocarbamic acid solution. Antimony(III) chloride was added slowly to the solution with vigorous stirring. The pale yellow precipitate was separated from the solution, washed with water and allowed to evaporate. The obtained product was recrystallized to get an excellent yield (**Scheme-I**). Yield: 82%, m.p.: 169 ºC. Anal. calcd. (found) % for $C_{39}H_{36}N_3O_3S_6Sb$ (908.87): C, 51.54 (51.49); H, 3.99 (3.91); N, 4.62 (4.58). IR (KBr, cm^{-1}): Experimental: 1463 ν(C-N), 1009 ν(C-S), 2849 ν(C-H), Theoretical: 1487.33 ν(C-N), 1009.28 ν(C-S), 3063.42 ν(C-H), ^{1}H NMR (400 MHz, $CDCl_3$, ppm): Experimental: 5.09 (6H, N-CH_2-C_6H_5); 5.15 (6H, s, CH_2 furfuryl) ; 6.30-7.35 (arom. protons); Theoretical: 3.6127 (20H) (N-CH_2-C_6H_5); 4.6962 (23H) (6H, CH_2 furfuryl); 6.3797-7.5354 (42H-6.3797) (44H-6.3797) (73H-7.1978) (75H-7.2805) (76H-7.1978) (77H-7.1978) (45H-7.5354) (71H-7.5354) (arom. protons): ^{13}C NMR (100 MHz, $CDCl_3$, ppm); Experimental: 48.03 (CH_2-C_6H_5); 55.6 (CH_2 furfuryl), 110.5,110.8,142.3, 148.5 (furyl ring carbons); 128.06, 128.15, 128.21, 134.5 (phenyl ring carbons) 204.3 (NCS_2): Theoretical: 53.9788 (19C) (CH_2-C_6H_5); 42.0635 (17C) (CH_2 furfuryl), (41C-105.5030) (39C-106.5899) (43C-141.6972) (38C-151.2030) (furyl ring carbons); (74C-121.5154) (72C-122.0282) (70C-123.1487) (68C-124.3711) (69C-125.0117) (67C-128.4825) (phenyl ring carbons) 222.9141 (16C) (NCS2).

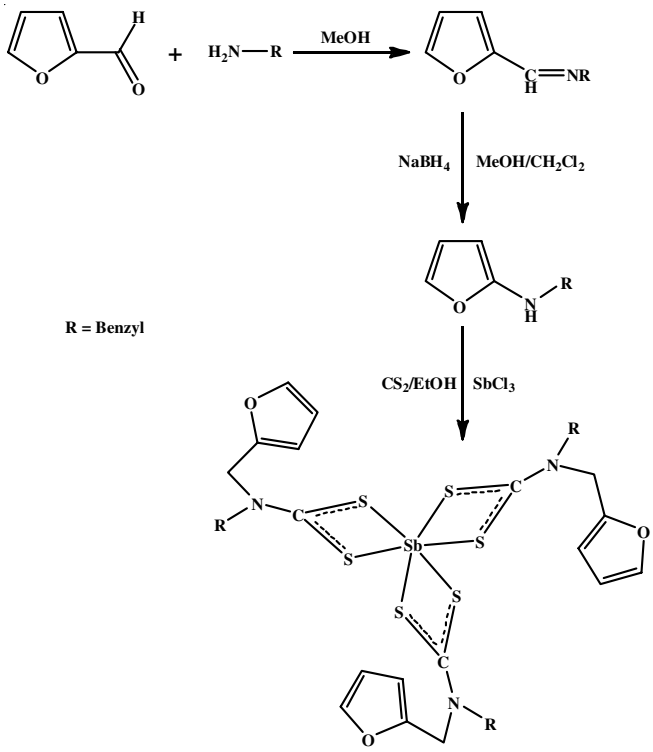

Scheme-I: Preparation of complex **1**

Computation procedures: All the quantum chemical calculations were performed at the density functional theory by using the functional B3LYP (Becke's three-parameter hybrid functional using LYP correlation functional) with LANL2DZ basis set using Gaussian 09 W package [50]. The mainly optimized structural parameters such as bond distance, bond angle and dihedral angle were calculated from Gaussian 09 W program. The vibrational frequencies and molecular geometry optimization of the antimony dithiocarbamate complex were calculated. The ^{1}H & ^{13}C NMR spectra were performed at DFT using the GIAO [51,52] methods using chloroform solvent with TMS as reference. The molecular optimized structures of the complex have been used to calculate the highest occupied molecular orbital and lowest unoccupied molecular orbital [53] plots were visualized using Gauss View 5.0. Global softness (S), energy gap, electrophilicity, global hardness, electrophilicity index (ω), Mulliken charge distribution of atoms [54] of systems were performed using Gauss View 5.0. The nucleophilic and electrophilic regions were visualized by molecular electrostatic potential was visualize using Gauss View 5.0 [55]. In addition, many other parameters like total energy, molecular dipole moment parameters were tabulated.

Antimicrobial activity: Mueller Hinton Agar-well disc diffusion [56] assay was used to determine the antimicrobial activity of the dithiocarbamate complex using Gram-positive and Gram-negative strains of bacteria (*Staphylococcus aureus*, *Vibrio cholerae*, *Klebsiella pneumonia*, *Escherichia coli)* and fungal (*Candida albicans* and *Aspergillus niger*). Disc plates were prepared by adding 10 mL of autoclaved Muller-Hinton Agar-well into sterile plates (900 mm) and allowing them to settle. Sterile blank discs (0.6 cm) were impregnated with 15 µL of known concentration of stock solution of the tested complex to obtain discs containing different concentrations of 400 and 800 µg of complex **1**. Impregnate discs were air-dried and carefully placed on the surface of Muller-Hinton Agar-well plates freshly inoculated with microorganisms. The cultures of the microorganism were arranged in a sterile nutrient broth medium and incubated at 37 ºC for 24 h for bacteria and 27 ºC for fungal when inhibition or clear zones are detected in the region of each hole. The spread plates were incubated for 24 h. Commercial ciprofloxacin impregnated disc was used as a reference drug for the comparison of microorganisms.

RESULTS AND DISCUSSION

Infrared analysis: Infrared spectroscopy has been used to know the nature of the monodentate or bidentate coordination mode of dithiocarbamate complex **1**. The decisive factor, the presence of one attribute band in the region 1050-900 cm^{-1}, the ν(C-S) mode, is due to the bidentate coordination mode of the dithiocarbamate moiety while a split band within the narrow range of 20 cm^{-1} indicates the monodentate nature of the dithiocarbamate moiety [57,58]. The C-S stretching vibrations are observed at 1017 cm^{-1} without any splitting, supporting the bidentate coordination mode of the dithiocarbamate ligand, whereas computational calculation bands at 1019.11 cm^{-1} using B3LYP theoretical method. The second lies in between 1600-1450 cm^{-1}, which is attributed to the thioureide ν(C-N) band [59]. This thioureide band may be considered as an intermediate between double and single bond C–N and its bond position indicate the shift of electron density towards the metal ion. Antimony dithiocarbamate complex band appeared at 1470 cm^{-1} is due to thioureide ν(C-N), which were computationally calculated as 1465.2121 cm^{-1} using LANL2DZ basis set using the Gaussian 09W package. The M-S stretching bands for the dithiocarbamate complex are usually in the range 300-400 cm^{-1} and that could not be measured due to the IR spectral range of the measurements. The infrared spectrum of antimony dithiocarbamate complex **1** is shown in Fig. 1.

NMR studies: ^{1}H NMR and ^{13}C NMR spectra of complex **1** are given in Fig. 2. In the ^{1}H NMR spectrum of complex, the presence of proton resonances for the dithiocarbamate ligand confirms the formation of metal complex. In ^{1}H NMR spectrum of complex, two singlets are obtained in the region of 5.09-5.15 ppm experimentally which were found at 3.6127-4.6962 ppm based on the theoretical spectrum using gauge-invariant atomic orbital (GIAO) method [60], for the CH_2 protons of furfuryl and benzyl group. Among these two signals, the downfield signal is usually attributed to protons of the furfuryl CH_2 group. This is due to the resonance effect of furfuryl ring. The aromatic protons of phenyl and furfuryl are obtained in the downfield region 6.0-7.35 ppm, which were theoretically calculated in the range 6.3797-7.5354 ppm.

Tris(*N*-furfuryl-*N*-benzyldithiocarbamato-S,S′)antimony (III) exhibited two signals, one at 48.03 ppm and other signal

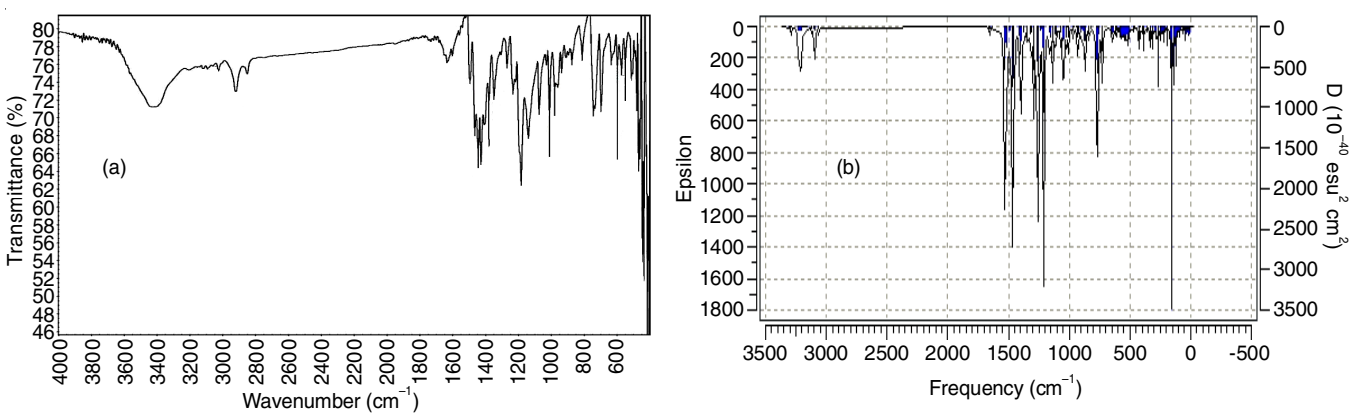

Fig. 1. Experimental (a) and computational (b) infrared spectra of complex **1**

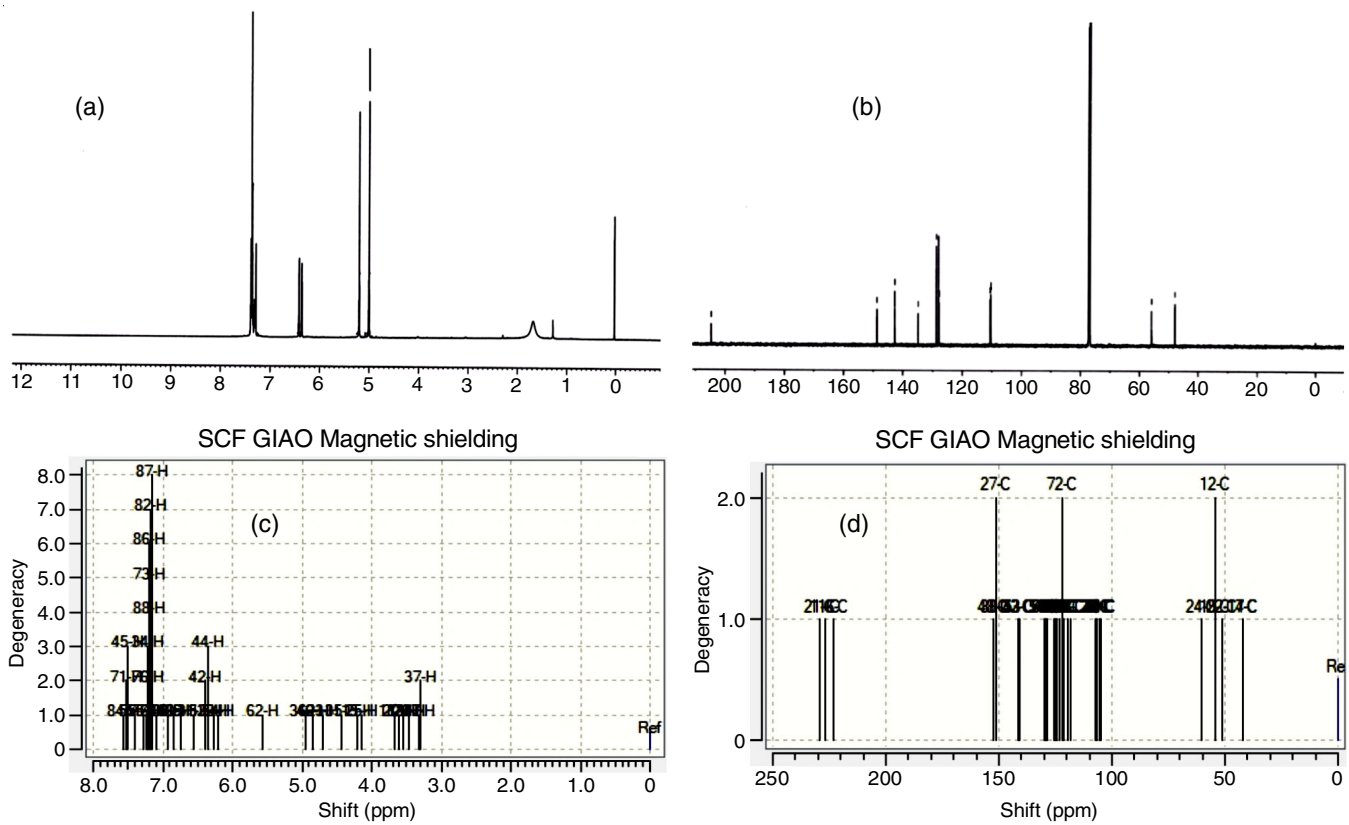

Fig. 2. Experimental (up) and computational (down) NMR spectra of complex **1**. [(a)(b)-^{1}H and (c) (d) ^{13}C NMR for complex **1**]

at 55.6 ppm due to methylene carbons of benzyl and furfuryl and which were theoretically obtained at δ 53.9788 ppm and δ 42.0635 ppm, respectively. The significant ^{13}C NMR signal of the $N^{13}CS_2$ carbons are obtained at 204.3 ppm for complex **1**, with a very weak intensity characteristic of quaternary carbon signals, which point to the bidentate character of dithiocarbamate ligand [61], which were found at δ 222.9141 ppm based on the theoretical spectrum of antimony dithiocarbamate of title complex.

Optimized structure: The optimized molecular structure of antimony dithiocarbamate complex **1** is shown in Fig. 3. The energy and dipole moment of the dithiocarbamate complex **1** were -1963.4520 eV and 3.3037 eV, respectively. The role of optimized molecular structural parameters selected bond length, bond angle and dihedral angle for the dithiocarbamate complex **1**. The calculated selected geometric parameters of *tris*(*N*-furfuryl-*N*-benzyldithiocarbamato-S,S′)antimony(III) has own nearly 15 bond length, 15 bond angle and 15 dihedral angle as listed in Table-1. The lone pair electrons of Sb lie trans to the Sb1-S5 (3.05409 Å) bond. In this complex, Sb adopts a distorted pentagonal pyramid due to its stereochemically active lone pair electrons. It is evident that longer Sb···S intermolecular interactions (2.61825 Å and 3.05409 Å) are also present resulting in a centrosymmetric bridged binuclear complex. The C-N and C-S bond distances in the structure of antimony dithiocarbamate complex **1** lies between 1.35193-1.35799 Å (C16-N9, C11-N8 and C21-N10) and 1.75665-1.82788 Å (C16-S5, C21-S7, C11-S3, C11-S2, C21-S6 and C16-S4), respectively. The short thioureide C-N bond lengths are in the

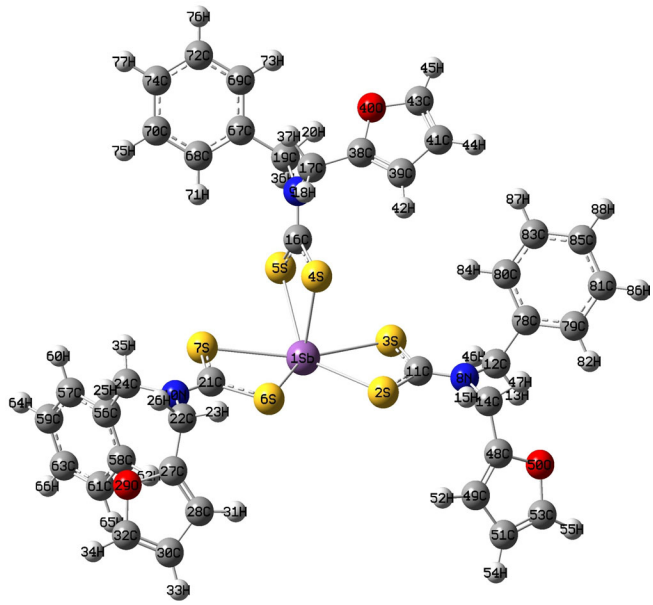

Fig. 3. Optimized structure with atoms numbering of complex **1**

range 1.35193-1.35799 Å, which evidently indicates delocalized electron density over the S_2CN moiety and this bond has a partial double bond nature. The C–S distances (mean: 1.79024 Å) are an intermediate value between the single and double bond distances, representing partial double bond character [62-67]. The bond angle and torsional angle of the complex **1** were found at 65.37234° (S4-Sb1-S5) and -177.17306° (S6-C21-N10-C24), respectively.

TABLE-1
SELECTED BOND LENGTH (Å), BOND ANGLE (°) AND DIHEDRAL ANGLES (°) FOR COMPLEX **1**

Bond distances (Å)		Bond angles (°)		Dihedral Angles (°)	
S2-Sb1	2.81121	S2- Sb1-S3	64.37293	S6-C21-N10-C24	-177.17306
S3- Sb1	2.96746	S4- Sb1-S5	65.37234	S7-C21-N10-C22	-171.71668
S4- Sb1	2.61825	S6- Sb1-S7	64.36028	N10-C24-C56-C57	-154.42937
S5- Sb1	3.05409	S3- C11-S2	118.60520	N10-C22-C27-C28	-154.42937
S6- Sb1	2.81152	S3- C11-N8	122.02363	H35-C24-C56-C58	150.98927
S7- Sb1	2.96973	S2- C11-N8	119.36417	S2-C11-N8-C12	176.67875
C11-S2	1.80628	C12-N8- C14	114.47365	S3-C11-N8-C14	177.34224
C11-S3	1.77675	S4- C16-S5	118.77397	N8-C12-C78-C79	111.06513
C11-N8	1.35333	S4- C16-N9	117.43533	N8-C14-C48-C49	-93.60331
C16-S4	1.82788	S5- C16-N9	123.79055	H13-C12-C78-C80	170.75996
C16-S5	1.75665	C17-N9- C19	114.58296	S5-C16-N9-C17	179.11462
C16-N9	1.35193	S6- C21-S7	119.15571	S4-C16-N9-C19	176.28676
C21-S6	1.80669	S6- C21-N10	119.52149	N9-C17-C38-C39	-95.37922
C21-S7	1.76721	S7- C21-N10	121.31611	N9-C19-C67-C69	115.97003
C21-N10	1.35799	C22-N10- C24	116.48774	H75-C68-C67-C19	115.97003

Frontier molecular orbitals (FMOs): The FMOs are a vital predictor of the molecular reactivity and polarizability of a molecule. A wide range of chemical reactions take place through the transfer of electron density from the highest occupied molecular orbital to the lowest unoccupied molecular orbital and are facilitated by a decrease in the HOMO-LUMO gap as the arrangement proceeds towards a transition state [68]. The HOMO-LUMO gap reflects the chemical activity of the compound [69-72]. Frontier molecular orbitals (FMO) calculations were carried out by DFT/B3LYP with LANL2DZ as a basis set. The energy difference between these frontier molecular orbital's play a vital role as an analytical parameter and understanding molecular transport properties The distributions of the highest occupied molecular orbital and lowest unoccupied molecular orbitals are computed at the same level of theory and are shown in Fig. 4. It is observed that the HOMO is mainly localized on the sulfur atoms and LUMO is localized on the Sb, C of CS_2 and N atoms of the molecule. In addition, it is important to note that both the electron-withdrawing group and the electron attracting group affect the chemical activity of the molecule. It is helpful to remind that small energy gaps are usually connected with low kinetic stability, high chemical reactivity and that these molecules are termed soft molecules [73]. In this present work, the energy difference between the highest occupied molecular orbital and lowest unoccupied molecular orbitals was calculated as 3.8016 eV in the gas phase. The global chemical reactivity descriptors of molecules like global hardness (η), global softness (S), electronic chemical potential (μ), electronegativity (χ) and electrophilicity index(ω) can be described *via* using the highest occupied molecular orbital and lowest unoccupied molecular orbital energies of molecule [74] at B3LYP/LANL2DZ basis are given in Table-2.

According to Koopman's theorem [75], the ionization potential (IP) and electron affinity (EA) are represented as IP = $-E_{HOMO}$ = 5.8487 eV and EA = $-E_{LUMO}$ = 2.0471 eV, respectively. The global hardness (η) which related to the reactivity and stability of a molecule and Mulliken electronegativity (χ) can be calculated as: η = ½ (E_{LUMO}-E_{HOMO}) = 1.9008 eV and χ = -½ (E_{HOMO} + E_{LUMO}) = 3.9479 eV, respectively. The global hardness (η) is a measure of the resistance of an atom to charge transfer of moiety [76]. The global softness (S) can be computed S = 1/2η = 0.2630 eV and represents the ability of a molecule to receive the electrons. The electrophilicity index (ω) can be calculated from Mulliken electronegativity and chemical hardness as follows: ω = $\mu^2/2\eta$ = 4.0998 eV and determines the

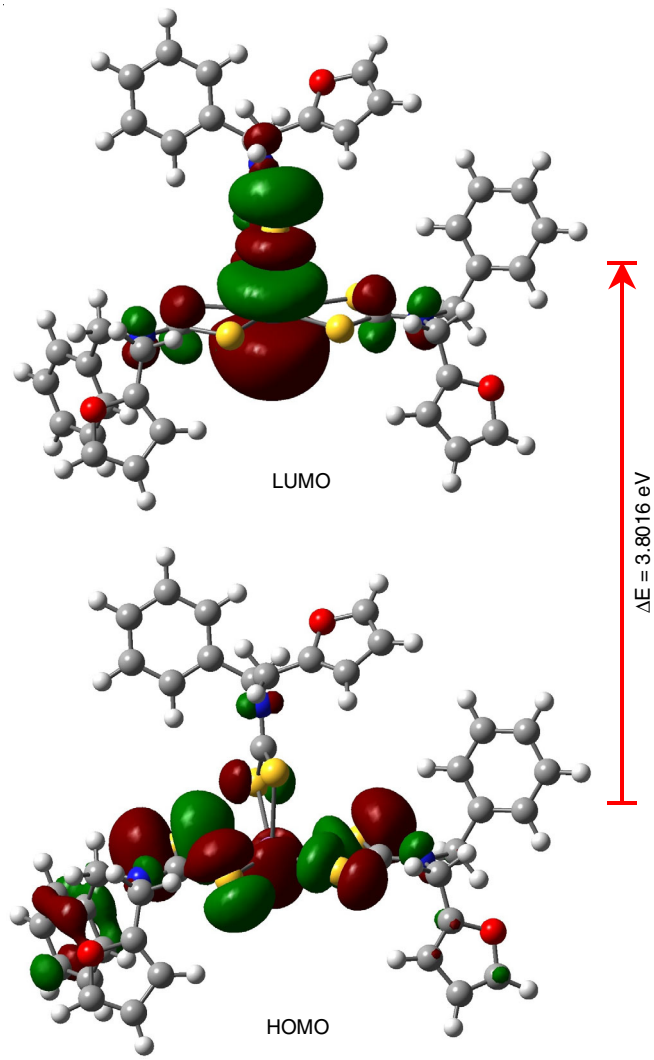

Fig. 4. HOMO and LUMO plots of complex **1**

TABLE-2
CALCULATED FMOs AND RELATED
MOLECULAR PROPERTIES OF COMPLEX **1**

Parameters	eV
HOMO	-5.8487
LUMO	-2.0471
Energy gap	3.8016
Ionization potential (IP)	5.8487
Electron affinity (EA)	2.0471
Global hardness (η)	1.9008
Chemical potential (μ)	-3.9479
Electronegativity (χ)	3.9479
Global softness (S)	0.2630
Electrophilicity index (ω)	4.0998
Energy	-1963.4520
Dipole moment (Debye)	3.3037

stabilization energy of the chemical moiety [77,78]. The electrophilicity index (ω) is a measure of energy lower due to the maximal electron flow between the acceptor and donor. The electrophilicity index of the title molecule is 4.0998 eV in the gas phase ensures strong energy transformation between HOMO and LUMO. The electronic chemical potential m is the negative of Mulliken electronegativity. The electronegativity is observed to be 3.9479 eV. Electronegativity (χ) is a measure of the attraction of an atom/group for electrons in a covalent bond. When two dissimilar atoms are covalently bonded, the shared electrons will be more powerfully attracted to the atom of better electronegativity. The values of global hardness (η), chemical potential (μ), electronegativity (χ), global softness (S) and electrophilicity index (ω) for complex **1** are 1.9008 eV, -3.9479 eV, 3.9479 eV, 0.2630 eV and 4.0998 eV in the gas phase by DFT/B3LYP with LANL2DZ as a basis set, respectively.

Molecular electrostatic potential: The MEP surface analysis of the complexes was determined by the DFT calculation using the optimized structures with B3LYP theory measure with LANL2DZ base set. MEP energy illustrates information regarding the charge distribution of a molecule. The potential has been mainly useful as an indicator of the sites or regions of a molecule to which an approaching nucleophile and electrophile is primarily attracted. The molecular electrostatic potential (MEP) is associated with the electronic density and very useful descriptor for a formative zone for electrophilic attack and nucleophilic site as well as H-bonding interactions. The reactive site for nucleophilic and electrophilic attack for complex **1** is shown in Fig. 5. With molecular electrostatic potential analysis, the reactive sites are positioned by different colour codes. A molecular electrostatic potential map helps to visualize charge-related properties and charge distribution of the molecules. The red colour in the MEP graphic indicates an electron-rich site, which is a negative region showing electrophilic reactivity. The blue colour in the MEP map indicates an electron-deficient zone, which is a positive region that shows nucleophilic reactivity [79]. The green colour in the MEP plots indicates the zero neutral, electrostatic potential zone showing hydrogen bonding interactions. The colour code of molecular electrostatic potential maps is the range between -4.475 e^{-2} (red) to +4.475 e^{-2}. (blue) in complex **1**.

Generally, the negative potential sites were localized over the area of a highly electron-rich zone. As can be seen from the negative a region was mainly concentrated over the portion of oxygen and nitrogen indicating a possible site for electrophilic attacks. An extreme maximum positive region is localized on the hydrogen atoms indicating an acceptable site for nucleophilic attacks. The depletion zone was neither positive nor negative potential atom of the molecule. The contour maps are a two-dimensional illustration of the regions where the values of the virtual electron density lie within a range. The electron-rich lines (red) are around oxygen and nitrogen whereas electron-deficient lines are shown by greenish-yellow lines. The contour map of surface-displayed in Fig. 5 and contour map performed at 0.004 density with the same level of calculation in complex **1**. The contour plots are used to show lines

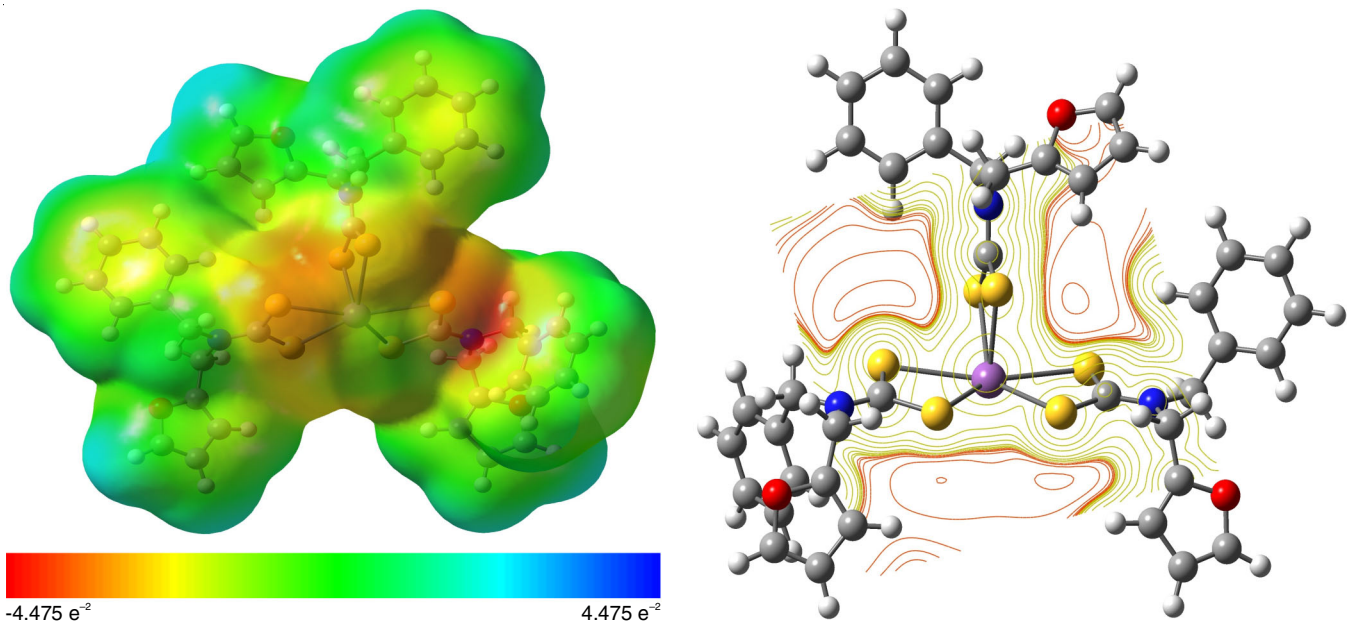

Fig. 5. Molecular electrostatic potential surface and contour map of complex **1**

of stable brightness, such as MEP and are drawn in the molecular plane.

Mulliken atomic charges: The charge transfer and atomic charges concept define molecular behaviour and reactivity and consequently, analysis of atomic charges plays a vital role in quantum chemical calculation. The atomic charges on the atoms are calculated by Mulliken population study *via* DFT/B3LYP methods with LANL2DZ basis level. Mulliken charge distribution of graphical representation is displayed in Fig. 6 and values are listed in Table-3. It is observed that there are closed contours for all oxygen atoms and present each of the furfuryl rings. All Hydrogen atoms were showed a net positive charge on H52 = 0.276295, H42 = 0.277069 and, H31 = 0.277864 atoms are greater than those of the other atoms due to the presence of electron-withdrawing group near these atoms such as oxygen and nitrogen atoms. The Mulliken charge distribution on 39 carbon atoms were exhibited either negative (C12 = -0.53509) or positive (C78 = 0.491704) values. These values point out the nature of the meticulous atoms and their effects on the vibratory frequencies of the molecule. These charges are associated with the dipole moment, electronic structure, chemical reactivity, polarizability and other properties of the molecule. Natural charges are calculated by summing the tenancy of natural atomic orbitals [80] and are much more consistent than that of Mulliken charges. Antimony atom has a maximum positive charge of Sb1 = 0.920771.

Antimicrobial activity: The antimicrobial activity of the title complex was assayed at the concentrations of 400 and 800 μg mL^{-1} against four bacterial and two fungal species.

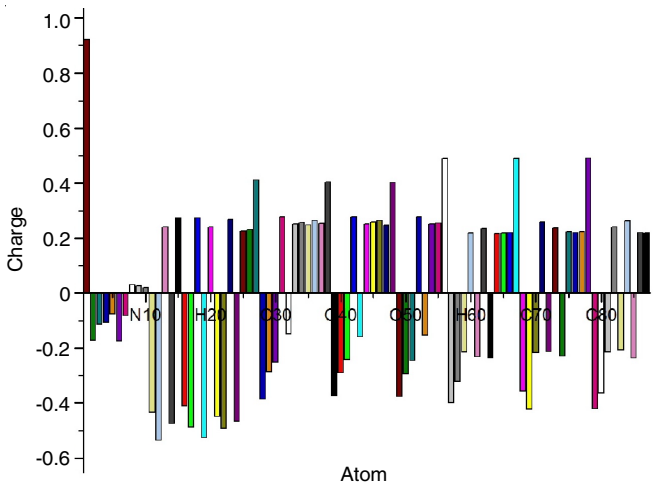

Fig. 6. Mulliken charge distribution of graphical representation of complex **1**

The inhibitory effects of complex **1** against bacteria and fungi are summarized in Table-4. Ciprofloxacin was used as a standard drug. The activity of complex **1** is lower than those of the reference drug used. The impact of central metal atom of complex **1** was found in the antimicrobial activity against the tested bacterial and fungal species. The results observed by the disk diffusion method indicated that the coordinated antimony(III) atom increases the antimicrobial activity. The effect is, as predictable, proportional to the concentration of the complex **1**. Antimony dithiocarbamate complex **1** is a good antimicrobial agent for certain bacterial and fungi. The title complex was demonstrated lower antibacterial activity against

TABLE-3
CALCULATED MULLIKEN ATOMIC CHARGE DISTRIBUTION OF COMPLEX **1**

Atom	Charge	Atom	Charge	Atom	Charge	Atom	Charge	Atom	Charge
Sb1	0.920771	C19	-0.52421	H37	0.252829	H55	0.25599	H73	0.236938
S2	-0.17359	H20	0.240851	C38	0.405299	C56	0.488708	C74	-0.2293
S3	-0.11428	C21	-0.44995	C39	-0.37375	C57	-0.39958	H75	0.222874
S4	-0.10677	C22	-0.49113	O40	-0.29107	C58	-0.32276	H76	0.220654
S5	-0.07694	H23	0.267616	C41	-0.24214	C59	-0.21443	H77	0.223456
S6	-0.17395	C24	-0.46685	H42	0.277069	H60	0.217544	C78	0.491704
S7	-0.08149	H25	0.225867	C43	-0.15939	C61	-0.23086	C79	-0.42183
N8	0.030691	H26	0.231634	H44	0.250648	H62	0.23561	C80	-0.36378
N9	0.02562	C27	0.411859	H45	0.258331	C63	-0.23746	C81	-0.21438
N10	0.018984	C28	-0.38587	H46	0.264551	H64	0.217212	H82	0.240069
C11	-0.43409	O29	-0.28751	H47	0.245627	H65	0.218315	C83	-0.20747
C12	-0.53509	C30	-0.25208	C48	0.403123	H66	0.22012	H84	0.261985
H13	0.239547	H31	0.277864	C49	-0.37769	C67	0.489582	C85	-0.23676
C14	-0.47381	C32	-0.14845	O50	-0.29386	C68	-0.35683	H86	0.220041
H15	0.273757	H33	0.25183	C51	-0.24628	C69	-0.42446	H87	0.218306
C16	-0.41093	H34	0.257203	H52	0.276295	C70	-0.21785		
C17	-0.48635	H35	0.246802	C53	-0.15441	H71	0.257941		
H18	0.27312	H36	0.264944	H54	0.250824	C72	-0.21259		

TABLE-4
ANTIMICROBIAL ACTIVITY (DIAMETER OF INHIBITION ZONE) OF COMPLEX **1**

Complex	Disc content (μg)	Selected bacteria				Selected fungal	
		V. cholera	*S. aureus*	*K. pneumoniae*	*E. coli*	*C. albicans*	*A. niger*
	400	09	06	05	07	05	08
	800	15	13	11	13	09	16
Ciprofloxacin		35	26	34	35	35	26

Klebsiella pneumoniae than those of other bacterial and better antibacterial activity against *Vibrio cholerae*. The antifungal studies revealed that better activity against *Aspergillus Niger* than *Candida albicans*. The functionalization of N-bound organic moiety of dithiocarbamate ligands in antimony (III) complex does not affect the antibacterial and antifungal activity of antimony(III) dithiocarbamate complex **1**.

Conclusion

The characterization study of *tris*(*N*-furfuryl-*N*-benzyl-dithiocarbamato-S,S′)antimony(III) complex **1** was carried out at B3LYP method in the Gaussian 09 program together with the LANL2DZ basis level using density functional theory. The infrared, ^{1}H NMR, ^{13}C NMR, HOMO-LUMO, energy gap, bond lengths, bond angles, dihedral angles and various other properties for the optimized molecule have been computed with DFT. The ^{1}H NMR and ^{13}C NMR spectra were calculated by the gauge independent atomic orbital (GIAO) approach at the same level of theory. The frontier molecule orbital analysis of the title complex was performed and the respective HOMO-LUMO plots were drawn. The centers of nucleophilic and electrophilic regions were identified by calculating the molecular electrostatic potential (MEP). Molecular behaviour and reactivity are revealed by Mulliken atomic charge distribution. The discrepancies between experimental and theoretical values are found due to fact that the experimental calculations have been carried out for that the molecule is in solid phase while theoretical calculations belong to the gaseous phase. The antimicrobial results observed by the disk diffusion method indicated that the coordinated antimony(III) atom increases the antimicrobial effects. The functionalization of the N-bound organic moiety of complex does not affect the antibacterial and antifungal activity of antimony(III) dithiocarbamate.

CONFLICT OF INTEREST

The authors declare that there is no conflict of interests regarding the publication of this article.

REFERENCES

1. L.G. Oliveira, M.M. Silva, F.C.S. Paula, E.C. Pereira-Maia, C.L. Donnici, C.A. Simone, F. Frézard, E.N.S. Júnior and C. Demicheli, *Molecules*, **16**, 10314 (2011); https://doi.org/10.3390/molecules161210314
2. F. Frezard, C. Demicheli, K.C. Kato, P.G. Reis and E.H. Lizarazo-Jaimes, *Rev. Inorg. Chem.*, **33**, 1 (2013); https://doi.org/10.1515/revic-2012-0006
3. R.N. Duffin, M.V. Werrett and P.C. Andrews, *Adv. Inorg. Chem.*, **75**, 207 (2020); https://doi.org/10.1016/bs.adioch.2019.10.001
4. S.K. Hadjikakou, D.C. Antoniadis, N. Hadjiliadis, M. Kubicki, J. Binolis, S. Karkabounas and K. Charalabopoulos, *Inorg. Chim. Acta*, **358**, 2861 (2005); https://doi.org/10.1016/j.ica.2004.06.028
5. E.R.T. Tiekink, *Crit. Rev. Oncol. Hematol.*, **42**, 217 (2002); https://doi.org/10.1016/S1040-8428(01)00217-7
6. S. Yan, F. Li, K. Ding and H. Sun, *J. Biol. Inorg. Chem.*, **8**, 689 (2003); https://doi.org/10.1007/s00775-003-0468-1
7. J.O. Adeyemi and D.C. Onwudiwe, *Molecules*, **25**, 305 (2020); https://doi.org/10.3390/molecules25020305
8. S.K. Hadjikakou, I.I. Ozturk, C.N. Banti, N. Kourkoumelis and N. Hadjiliadis, *J. Inorg. Biochem.*, **153**, 293 (2015); https://doi.org/10.1016/j.jinorgbio.2015.06.006
9. K. Gleu and R. Schwab, *Angew. Chem.*, **62**, 320 (1950); https://doi.org/10.1002/ange.19500621307
10. A. Hulanicki, *Talanta*, **14**, 1371 (1967); https://doi.org/10.1016/0039-9140(67)80159-0
11. A.T. Pilipenko and N.V. Ul'ko, *Chem. Abstr.*, **50**, 2356 (1956).
12. E.R.T. Tiekink, *Appl. Organomet. Chem.*, **22**, 533 (2008); https://doi.org/10.1002/aoc.1441
13. P.J. Heard, *Prog. Inorg. Chem.*, **53**, Chap. 1 (2005); https://doi.org/10.1002/0471725587.ch1
14. D. Coucouvanis, *Prog. Inorg. Chem.*, **26**, 301 (1979).
15. G. Hogarth, *Prog. Inorg. Chem.*, **53**, 71 (2005); https://doi.org/10.1002/0471725587.ch2
16. J. Willemse, J.A. Cras, J.J. Steggerda and C.P. Keijzers, *Struct. Bonding*, **28**, 83 (1976); https://doi.org/10.1007/3-540-07753-7_3
17. J.J. Steggerda, J.A. Cras and J. Willemse, *Recl. Trav. Chim. Pays Bas*, **100**, 41 (1981); https://doi.org/10.1002/recl.19811000202
18. A.M. Bond and R.L. Martin, *Coord. Chem. Rev.*, **54**, 23 (1984); https://doi.org/10.1016/0010-8545(84)85017-1
19. H.Y. Li, C.S. Lai, J.Z. Wu, P.C. Ho, D. de Vos and E.R.T. Tiekink, *J. Inorg. Biochem.*, **101**, 809 (2007); https://doi.org/10.1016/j.jinorgbio.2007.01.010
20. R.Z. Sun, Y.C. Guo, W.M. Liu, S.Y. Chen and Y.Q. Feng, *Chin. J. Struct. Chem.*, **31**, 655 (2012).
21. H.P. Chauhan, A.A. Bakshi and S. Bhatiya, *Spectrochim. Acta A Mol. Biomol. Spectrosc.*, **81**, 417 (2011); https://doi.org/10.1016/j.saa.2011.06.031
22. H.P.S. Chauhan and U.P. Singh, *Appl. Organomet. Chem.*, **21**, 880 (2007); https://doi.org/10.1002/aoc.1290
23. H. Yin, F. Li and D. Wang, *J. Coord. Chem.*, **60**, 1133 (2007); https://doi.org/10.1080/00958970601008846
24. H.P.S. Chauhan, N.M. Shaik and U.P. Singh, *Appl. Organomet. Chem.*, **20**, 142 (2006); https://doi.org/10.1002/aoc.1013
25. H.P.S. Chauhan, K. Kori, N.M. Shaik, S. Mathur and V. Huch, *Polyhedron*, **24**, 89 (2005); https://doi.org/10.1016/j.poly.2004.10.007
26. Y. Liu and E.R.T. Tiekink, *Appl. Organomet. Chem.*, **18**, 299 (2004); https://doi.org/10.1002/aoc.619
27. H.-D. Yin and C.-H. Wang, *Appl. Organomet. Chem.*, **18**, 420 (2004); https://doi.org/10.1002/aoc.671
28. H.-D. Yin, C.-H. Wang and Y. Wang, *Appl. Organomet. Chem.*, **18**, 199 (2004); https://doi.org/10.1002/aoc.597
29. C.S. Lai and E.R.T. Tiekink, *Appl. Organomet. Chem.*, **17**, 195 (2003); https://doi.org/10.1002/aoc.384
30. S.S. Garje and V.K. Jain, *Coord. Chem. Rev.*, **236**, 35 (2003); https://doi.org/10.1016/S0010-8545(02)00159-5
31. J. Rodriguez-Castro, P. Dale, M.F. Mahon, K.C. Molloy and L.M. Peter, *Chem. Mater.*, **19**, 3219 (2007); https://doi.org/10.1021/cm070405j
32. M.D. Regulacio, M.H. Pablico, J.A. Vasquez, P.N. Myers, S. Gentry, M. Prushan, S.W. Tam-Chang and S.L. Stoll, *Inorg. Chem.*, **47**, 1512 (2008); https://doi.org/10.1021/ic701974q
33. J.D.E.T. Wilton-Ely, D. Solanki, E.R. Knight, K.B. Holt, A.L. Thompson and G. Hogarth, *Inorg. Chem.*, **47**, 9642 (2008); https://doi.org/10.1021/ic800398b
34. M.D. Regulacio, N. Tomson and S.L. Stoll, *Chem. Mater.*, **17**, 3114 (2005); https://doi.org/10.1021/cm0478071
35. M. Becht, T. Gerfin and K.H. Dahmen, *Chem. Mater.*, **5**, 137 (1993); https://doi.org/10.1021/cm00025a026
36. C. Xu, T.H. Baum and A.L. Rheingold, *Chem. Mater.*, **10**, 2329 (1998); https://doi.org/10.1021/cm980346x
37. G.C. Wang, Y.N. Lu, J. Xiao, L. Yu, H.B. Song, J.S. Li, J.R. Cui, R.Q. Wang and F.X. Ran, *J. Organomet. Chem.*, **690**, 151 (2005); https://doi.org/10.1016/j.jorganchem.2004.09.002
38. O. Savadogo and K.C. Mandal, *Sol. Energy Mater. Sol. Cells*, **26**, 117 (1992); https://doi.org/10.1016/0927-0248(92)90131-8

39. X. Wang, K.F. Cai, F. Shang and S. Chen, *J. Nanopart. Res.*, **15**, 1541 (2013); https://doi.org/10.1007/s11051-013-1541-5
40. O.S. Urgut, I.I. Ozturk, C.N. Banti, N. Kourkoumelis, M. Manoli, A.J. Tasiopoulos and S.K. Hadjikakou, *Mater. Sci. Eng. C*, **58**, 396 (2016); https://doi.org/10.1016/j.msec.2015.08.030
41. I.I. Ozturk, C.N. Banti, N. Kourkoumelis, M.J. Manos, A.J. Tasiopoulos, A.M. Owczarzak, M. Kubicki and S.K. Hadjikakou, *Polyhedron*, **67**, 89 (2014); https://doi.org/10.1016/j.poly.2013.08.052
42. I.I. Ozturk, S. Filimonova, S.K. Hadjikakou, N. Kourkoumelis, V. Dokorou, M.J. Manos, A.J. Tasiopoulos, M.M. Barsan, I.S. Butler, E.R. Milaeva, J. Balzarini and N. Hadjiliadis, *Inorg. Chem.*, **49**, 488 (2010); https://doi.org/10.1021/ic901442e
43. I.I. Ozturk, O.S. Urgut, C.N. Banti, N. Kourkoumelis, A.M. Owczarzak, M. Kubicki, K. Charalabopoulos and S.K. Hadjikakou, *Polyhedron*, **52**, 1403 (2013); https://doi.org/10.1016/j.poly.2012.04.038
44. A.S. Levenson and V.C. Jordan, *Cancer Res.*, **57**, 3071 (1997).
45. R. Paridaens, L. Biganzoli, P. Bruning, J.G. Klijn, T. Gamucci, S. Houston, R. Coleman, J. Schachter, A. Van Vreckem, R. Sylvester, A. Awada, J. Wildiers and M. Piccart, *J. Clin. Oncol.*, **18**, 724 (2000); https://doi.org/10.1200/JCO.2000.18.4.724
46. J. Hoffmann, R. Bohlmann, N. Heinrich, H. Hofmeister, J. Kroll, H. Kunzer, R.B. Lichtner, Y. Nishino, K. Parczyk, G. Sauer, H. Gieschen, H.F. Ulbrich and M.R. Schneider, *J. Natl. Cancer Inst.*, **96**, 210 (2004); https://doi.org/10.1093/jnci/djh022
47. D.Y. Lu, M. Huang, C.H. Xu, W.Y. Yang, C.X. Hu, L.P. Lin, L.J. Tong, M.H. Li, W. Lu, X.W. Zhang and J. Ding, *BMC Pharmacol.*, **5**, 11 (2005); https://doi.org/10.1186/1471-2210-5-11
48. G.G. Mohamed, N.A. Ibrahim and H.E.A. Attia, *Spectrochim. Acta A Mol. Biomol. Spectrosc.*, **72**, 610 (2009); https://doi.org/10.1016/j.saa.2008.10.051
49. P.J. Rani and S. Thirumaran, *Eur. J. Med. Chem.*, **62**, 139 (2013); https://doi.org/10.1016/j.ejmech.2012.12.047
50. M.A. Mumit, T.K. Pal, M.A. Alam, M.A. Islam, S. Paul and M.C. Sheikh, *J. Mol. Struct.*, **1220**, 128715 (2020); https://doi.org/10.1016/j.molstruc.2020.128715
51. R. Ditchfield, *J. Chem. Phys.*, **56**, 5688 (1972); https://doi.org/10.1063/1.1677088
52. K. Wolinski, J.F. Hinton and P. Pulay, *J. Am. Chem. Soc.*, **112**, 8251 (1990); https://doi.org/10.1021/ja00179a005
53. H. Chermette, *J. Comput. Chem.*, **20**, 129 (1999); https://doi.org/10.1002/(SICI)1096-987X(19990115)20:1<129::AID-JCC13>3.0.CO;2-A
54. K. Ramirez-Balderrama, E. Orrantia-Borunda and N. Flores-Holguin, *J. Theor. Comput. Chem.*, **16**, 1750019 (2017); https://doi.org/10.1142/S0219633617500195
55. A. Zainuri, S. Arshad, N.C. Khalib and I.A. Razak, *J. Mol. Cry. Liq. Cryst.*, **650**, 87 (2017); https://doi.org/10.1080/15421406.2017.1328222
56. K. Chaturvedi, A. Kumar and A. Mishra, *Der Pharm. Chem.*, **6**, 27 (2014).
57. F. Bonati and R. Ugo, *J. Organomet. Chem.*, **10**, 257 (1967); https://doi.org/10.1016/S0022-328X(00)93085-7
58. J.O. Hill and R.J. Magee, *Rev. Inorg. Chem.*, **3**, 141 (1981).
59. J. Criado, I. Fernandez, B. Macias, J.M. Salas and M. Medarde, *Inorg. Chim. Acta*, **174**, 67 (1990); https://doi.org/10.1016/S0020-1693(00)80280-7
60. A.E. Aliev, D. Courtier-Murias and S. Zhou, *J. Mol. Struct. THEOCHEM*, **893**, 1 (2009); https://doi.org/10.1016/j.theochem.2008.09.021
61. H.L.M. Van Gaal, J.W. Diesveld, F.W. Pijpers and J.G.M. Van der Linden, *Inorg. Chem.*, **18**, 3251 (1979); https://doi.org/10.1021/ic50201a062
62. V. Venkatachalam, K. Ramalingam, G. Bocelli and A. Cantoni, *Inorg. Chim. Acta*, **261**, 23 (1997); https://doi.org/10.1016/S0020-1693(96)05573-9
63. K.Y. Low, I. Baba, Y. Farina, A.H. Othman, A.R. Ibrahim, H.K. Fun and S.W. Ng, *Main Group Met. Chem.*, **24**, 451 (2001); https://doi.org/10.1515/MGMC.2001.24.7.451
64. O.C. Monteiro, H.I.S. Nogueira, T. Trindade and M. Motevalli, *Chem. Mater.*, **13**, 2103 (2001); https://doi.org/10.1021/cm000973y
65. V. Venkatachalam, K. Ramalingam, U. Casellato and R. Graziani, *Polyhedron*, **16**, 1211 (1997); https://doi.org/10.1016/S0277-5387(96)00362-2
66. C.S. Lai and E.R.T. Tiekink, *Z. Kristallogr.*, **222**, 532 (2007); https://doi.org/10.1524/zkri.2007.222.10.532
67. R. Chauhan, J. Chaturvedi, M. Trivedi, J. Singh, K.C. Molloy, G. Kociok-Kohn, D.P. Amalnerkar and A. Kumar, *Inorg. Chim. Acta*, **430**, 168 (2015); https://doi.org/10.1016/j.ica.2015.03.007
68. N.J. Mosey, A. Hu and T.K. Woo, *Chem. Phys. Lett.*, **373**, 498 (2003); https://doi.org/10.1016/S0009-2614(03)00538-4
69. R.G. Pearson, *Proc. Natl. Acad. Sci. USA*, **83**, 8440 (1986); https://doi.org/10.1073/pnas.83.22.8440
70. H. Gokce, N. Ozturk, U. Ceylan, Y.B. Alpaslan and G. Alpaslan, *Spectrochim. Acta A Mol. Biomol. Spectrosc.*, **163**, 170 (2016); https://doi.org/10.1016/j.saa.2016.03.041
71. Z. Demircioglu, F.A. Ozdemir, O. Dayan, Z. Serbetci and N. Ozdemir, *J. Mol. Struct.*, **1161**, 122 (2018); https://doi.org/10.1016/j.molstruc.2018.02.063
72. G.O. Tari, U. Ceylan, E. Agar and H. Eserci, *J. Mol. Struct.*, **1126**, 83 (2016); https://doi.org/10.1016/j.molstruc.2016.01.058
73. Z.S. Sahin, G.K. Kantar, S. Sasmaz and O. Büyükgüngör, *J. Mol. Struct.*, **1087**, 104 (2015); https://doi.org/10.1016/j.molstruc.2015.01.039
74. R.G. Parr, L. Szentpaly and S. Liu, *J. Am. Chem. Soc.*, **121**, 1922 (1999); https://doi.org/10.1021/ja983494x
75. T. Koopmans, *Physica*, **1**, 104 (1934); https://doi.org/10.1016/S0031-8914(34)90011-2
76. R.G. Pearson, *J. Am. Chem. Soc.*, **107**, 6801 (1985); https://doi.org/10.1021/ja00310a009
77. H. Beg, S.P. De, Sankar, L. Ash and A. Misra, *Comput. Theoret. Chem.,* **984**, 13 (2012); https://doi.org/10.1016/j.comptc.2011.12.018
78. A. Srivastava, P. Rawat, P. Tandon and R.N. Singh, *Comput. Theoret. Chem.*, **993**, 80 (2012); https://doi.org/10.1016/j.comptc.2012.05.025
79. R.K. Singh, S.K. Verma and P.D. Sharma, *Int. J. Chem. Tech. Res.,* **3**, 1571 (2011).
80. M.J. Alam and S. Ahmad, *Spectrochim. Acta A Mol. Biomol. Spectrosc.*, **96**, 992 (2012); https://doi.org/10.1016/j.saa.2012.07.135